Algal Research 7 (2015) 33–44

Contents lists available at ScienceDirect

Algal Research

journal homepage: www.elsevier.com/locate/algal

Characterization of five fresh water microalgae with potential for biodiesel production

Ruby Valdez-Ojeda [a,*], Muriel González-Muñoz [a], Roberto Us-Vázquez [a], José Narváez-Zapata [c], Juan Carlos Chavarria-Hernandez [a], Silvia López-Adrián [d], Felipe Barahona-Pérez [a], Tanit Toledano-Thompson [a], Gloria Garduño-Solórzano [e], Rosa María Escobedo-Gracia Medrano [b]

[a] Unidad de Energía Renovable, Centro de Investigación Científica de Yucatán A.C., Mérida, Yucatán, Mexico
[b] Unidad de Bioquímica y Biología Molecular de Plantas, Centro de Investigación Científica de Yucatán A.C., Mérida, Yucatán, Mexico
[c] Centro de Biotecnología Genómica, Instituto Politécnico Nacional, Reynosa, Tamaulipas, Mexico
[d] Facultad de Veterinaria y Zootecnia, Universidad Autónoma de Yucatán, Mérida, Yucatán, Mexico
[e] Facultad de Estudios Superiores Iztacala, Universidad Autónoma de Mexico, Tlalnepantla, Edo. de México, Mexico

ARTICLE INFO

Article history:
Received 31 March 2014
Received in revised form 21 October 2014
Accepted 24 November 2014
Available online 10 December 2014

Keywords:
Scenedesmus
Desmodesmus
ITS-2
Fatty acids
Biodiesel properties
CBC analysis

ABSTRACT

Microalgae biodiesel feedstocks have been investigated by numerous research groups to overcome dependence on fossil fuels. This study describes a detailed characterization of five freshwater microalgae strains of the family Scenedesmaceae, based on cell wall ultrastructure, ITS-2 sequence and secondary structure analysis, as well as the estimation of biodiesel properties from fatty acids produced before and after N-limitation. Characterization permitted the reclassification of SCRE-1 and SCRE-2 strains into the subgenus *Scenedesmus*; DSRE-1 and DSRE-2 strains into the subgenus *Desmodesmus*; and CORE-1 strain into the genus *Coelastrum*. Transesterification of fatty acids of the five strains was performed before and after N-limitation, and seven important biodiesel quality parameters were predicted by applying selected correlations. These parameters were then compared to the corresponding specifications in the American and European biodiesel standards. N-limitation promoted higher yields of biomass (up to 3.5 times) and lipids (up to 4.1 times) in all strains under study. Moreover, it was found that SCRE-2 was the only biodiesel that met all estimated parameters of the more stringent European standard before N-limitation. This was also true for DSRE-1 and DSRE-2 biodiesels after limitation, with the exception of their oxidative stability parameter, whose values met the limit of the American but not the European standard.

1. Introduction

Microalgae (eukaryotes and prokaryotes) have attracted significant attention as renewable energy feedstocks due to their rapid biomass production and great potential to synthesize fatty acids suitable for biodiesel [1,2] compared to oleaginous plants [3]. The oil content of microalgae is usually between 10 and 50% of their dry cell weight, although some microalgae species can reach as high as 80% under certain conditions [4,5].

Species selection is one of the biggest challenges in biofuel production based on microalgae [6–8]. This selection is based principally on the fatty acid profile, which determines the main biodiesel properties, and thus the biodiesel quality. Some of the most important biodiesel properties include density, cetane number, kinematic viscosity, higher heating value, iodine value, cold flow plugging point, and oxidative stability. The density (ρ) of biodiesel is strongly influenced by temperature, and some quality standards have established limits for this property at 15 °C. The cetane number (CN) is a dimensionless descriptor related to the ignition quality of a fuel in a diesel engine. Generally, a higher CN value indicates a better ignition quality of the fuel and vice versa [9]. Kinematic viscosity (ν), on the other hand, affects the atomization of a fuel upon injection into the combustion chamber, and thereby ultimately the formation of engine deposits. The higher the viscosity, the greater the tendency of the fuel to cause such problems [10]. The iodine value (IV) is a measure of total unsaturation of an oil or fat. Biodiesels with high IV are easily oxidized in contact with air [11]. Gross heat of combustion (HG) or higher heating value (HHV) is another fuel property indicating the suitability of fatty compounds as diesel fuel. The presence of oxygen in the ester molecules decreases the heating value of biodiesel by 10 to 13% compared to that of diesel fuel. The HHV of petroleum diesels is around 45 MJ/kg, while that of biodiesels is around 40 MJ/kg. The cold filter plugging point (CFPP) is an estimate of the lowest temperature at which a fuel will give trouble-free flow in a given fuel system. Saturated fatty compounds have significantly higher melting points than unsaturated ones, and in a mixture they crystallize at higher temperature than unsaturated ones [11]. Crystals grow rapidly at low temperature and agglomerate, clogging filters partially or totally.

* Corresponding author.
E-mail address: ruby.valdez@cicy.mx (R. Valdez-Ojeda).

http://dx.doi.org/10.1016/j.algal.2014.11.009
2211-9264/

Countries using UNE-EN 14214 can select one of the two options (moderate or arctic climate) for seasonal classes (summer and winter) and modify this specification based on national meteorological data. The cloud point (CP) is the related property in ASTM D6751 for which an analogous limit is not given, rather a report is required. CFPP values are approximately 4.5 °C lower than CP values [12]. Finally, the oxidative stability (OSI) of biodiesel is an important issue for storage purposes, as the presence of double bonds in fatty esters greatly facilitates oxidation of biodiesel. Autoxidation of unsaturated fatty compounds proceeds at different rates depending on the number and position of double bonds. Relative rates of oxidation are 1 for oleates (methyl, ethyl esters), 41 for linoleates, and 98 for linolenates [10]. The species formed during the oxidation process eventually cause the fuel to deteriorate. Two types of tests are currently used for determining the oxidation stability of biodiesel: the Rancimat test, specified in EN 14214; and the oil stability index (OSI), included in ASTM D6751 [11]. As stated by [10], the Rancimat method is nearly identical to the oil stability index (OSI) method.

Suitable fatty acid profiles are usually associated with specific microalgae subgenera, such as *Scenedesmus* and *Desmodesmus*. In this context, C16–C18 fatty acids were found to account for over 98% of the fatty acid composition of *Scenedesmus obliquus*, indicating that biodiesel from these cells could meet biodiesel standards. Biodiesel quality from *S. obliquus* complied with the ASTM D6751 standard in terms of cetane number (>58), oxidative stability, degree of unsaturation and iodine value (<69) [13]. In another study, the fatty acid profile of *S. abundans*, with C16–C18 accounting for 90.6% of total FAMEs, showed biodiesel properties such as cetane number (52.15), iodine value (94.06 g I_2/100 g) and saponification value (202.02 mg KOH/g) in accordance with the specifications of the Brazilian National Petroleum Agency (ANP255) and the European biodiesel standard (EN 14214) [14].

A detailed review of the literature on fatty acid profiles from a wide range of microalgae species indicates that most of them contain C14:0, C16:0, C18:0, C18:1, C18:2 and C18:3 fatty acids [8,15]. For example, Vidyashankar et al. worked with five different strains, including *Scenedesmus* sp. and *Coelastrum asteroidum*, using CO_2 supplementation from 0.03 to 2% (v/v) [16]. These authors reported that the most abundant fatty acid methyl esters (FAMEs) obtained for the five strains at all CO_2 concentrations were C16:0, C18:0, C18:1, C18:2 and C18:3. For *Scenedesmus* sp., the amount of C16:0 + C18:1 was approximately 70% at all CO_2 percentages (v/v) tested, while the combined concentration of C16:0 + C18:1 for *C. asteroidum* amounted to approximately 80%. Reports on fatty acid profiles for microalgae of the subgenera *Desmodesmus*, *Coelastrum* and *Scenedesmus* indicate that the sum of C14:0 + C16:0 + C18:0 + C18:1 + C18:2 fatty acid concentrations usually represents between 80 and 90% of the total fatty acid content [7,13,14,17,18].

Biomass productivity and oil content are also important for screening microalgae species. In the work of Musharraf et al., *Desmodesmus* sp. WC08 showed higher biomass productivity (370 mg l/d) and higher lipid productivity (115.73 mg/l/d) than seven other microalgae species [7]. The main fatty acids synthesized by this microalga (C16–C18) indicated that it is suitable for biodiesel production [19]. In comparison with other microalgae species, such as *Chlorella*, *Haematococcus*, *Ulothrix*, *Chlorococcum*, *Rivularia* and *Scytonema*, the species *Scenedesmus* registered the highest lipid content (27.4% w/w) [20]. Similarly, in comparison with *Coelastrum* and *Ankistrodesmus*, *Scenedesmus* showed a high lipid content of 17.83% w/w [16]. Based on those and other reports, numerous authors have selected species of this genus mainly due to their potential for producing biofuel [21–25].

Scenedesmus belongs to the subfamily Scenedesmoideae from the family Scenedesmaceae, which includes other subgenera such as *Desmodesmus* and *Acutodesmus*, among others. Different species and strains of *Scenedesmus* and *Desmodesmus* have been studied and tested under different conditions in relation to their fatty acid production: e.g., higher light intensity to induce neutral as opposed to polar lipid synthesis [26]; nitrogen and phosphorous limitation to increase fatty acid synthesis [25]; and CO_2 fixation and light to enhanced production of fatty acids [27,28]. However, only a few microalgae cultures have been thoroughly examined in terms of cell structure and genetic classification in order to facilitate the identification of microalgae species with suitable fatty acid profiles for biodiesel. The study carried out by Kaur et al. [22] included the characterization of strains of *Scenedesmus* and *Desmodesmus* species based on ultrastructure and genetic analysis, as well as fatty acid determination to screen them for suitable fatty acid composition according to the ATSM D6751 (US) and UNE-EN 14214 (EU) international biodiesel standards.

Biodiesel property estimation for microalgae screening can be performed with good accuracy by applying different correlations reported in the literature. The main reason for this is that biodiesel is a mixture of a limited number of compounds (usually less than 10) belonging to the same family. Thus, for certain properties like density or cetane number, an ideal mixing rule can be good enough to calculate the mixture properties based on those of the individual compounds [29]. This methodology is especially helpful when the required analytical equipment or large enough amounts of oils are not available, but it is possible to determine the fatty acid composition. The presence of impurities (compounds other than fatty acid alkyl esters) will surely affect property estimation, but they are usually present in amounts lower than 5% by weight [30,31], so the interaction parameter considered in non-ideal mixing rules, such as in the Grunberg–Nissan equation [32], can be neglected.

According to the above, many authors have estimated and reported biodiesel properties by using different correlations available in the literature [29,33–35]. For the properties to be calculated, it is necessary to identify the fatty acid alkyl esters present in the mixture and the percentage or fractional amount of each one. The triglyceride source from which the biodiesel was obtained (i.e., vegetable oil, animal fat, microalgae oil, etc.) does not matter. There are many reports in the literature in which biodiesel quality has been estimated theoretically with the use of correlations. The properties most commonly estimated include the cetane number, viscosity, higher heating value, density, and cold flow properties such as the cloud point or the cold filter plugging point. The reported works include studies on the quality of biodiesel from microalgal oil [7,13–15,17,31,36].

Among the microalgae species that have been studied, subgenera *Desmodesmus* and *Scenedesmus* [37] are two strains showing extreme plasticity. Classification based on metabolic capability and morphology using optical microscopy has been found to be insufficient for clearly distinguishing between them [38,39]. The internal transcribed spacer-2 (ITS-2) region has been found to be useful as a molecular marker for resolving the evolutionary relationships among these closely related green algae, such as the subgenera *Desmodesmus* and *Scenedesmus* [40,41].

The main aim of this work was to investigate the potential of five strains for use as a source of microalgal oil for biodiesel production. This was performed by analyzing their cell wall ultrastructure, ITS-2 secondary structure and fatty acid profile. In order to investigate the quality of biodiesel from the five strains, the following seven important biodiesel properties were predicted by using selected correlations taken from the literature: density at 15 °C, cetane number, kinematic viscosity at 40 °C, higher heating value, iodine value, cold flow plugging point, and oxidative stability.

2. Materials and methods

2.1. Microalgal strains

Five strains from the subfamily Scenedesmoideae were studied. All of them were acquired from a national or international culture collection. Strain SCX2 (*Scenedesmus* sp.), labeled DRES-1 in this study, and strain SCX1 (*S. obliquus*), labeled SCRE-1, were acquired from the

Centro de Investigación Científica y de Educación Superior de Ensenada (CICESE) located in Baja California, Mexico. Strain CLHE-Si01 (*Scenedesmus incrassatulus*), labeled SCRE-2, was provided by the Escuela Nacional de Ciencias Biológicas (ENCB-IPN) located in Mexico City. Strain UADY-PRIORI-014-FMVZ-05 (*Scenedesmus* sp.), labeled CORE-1, was provided by the Facultad de Medicina Veterinaria y Zootecnia of the Universidad Autónoma de Yucatán, in Yucatan, Mexico. Strain KOVACIK 1983/3 (*Desmodesmus spinosus*), labeled DSRE-2, was acquired from the Culture Collection of Autotrophic Organisms (CCALA). All microalgae were first plated on Bold's Basal semisolid culture medium for microalgae cell maintenance and kept under controlled culture conditions (27 °C, 16:8 light–dark, and light intensity of 100 μmol/m^2/s). Growth curves for each microalga were carried out in 50 ml Erlenmeyer flasks containing 10 ml fresh TAP medium [42] for heterotrophic conditions, which can significantly increase growth rates, cell mass and protein and lipid productivities [43], using an initial cell concentration of 10,000 cell/ml. They were incubated at 27 ± 2 °C, 120 rpm, and a light intensity of 100 μmol/m^2/s with a 16:8 (light/dark) photoperiod. Samples were taken every day (500 μl) and cell concentration was determined using a Neubauer hemocytometer.

2.2. Scanning electron microscopy (SEM) analysis

For SEM analysis, 200 mg of microalgal cells in stationary phase was recovered and centrifuged at 9727 ×*g* for 20 min. The supernatant was discarded and the pellet was kept in desiccators under vacuum for 24 h in 2.5% glutaraldehyde at 4 °C. This procedure was repeated three times to guarantee cell fixation. Fixation agent was then removed by centrifugation at 9727 ×*g* for 20 min. The pellet was subsequently washed six times in 0.2 M pH 7.1 phosphate buffers. Sequential dehydration was performed in an ethanol series (30%, 40%, 55%, 70%, 85%, and 100%) at 4 °C. Individual samples were deposited into microporous specimen capsules to be dried using a Samdri 795 Semi Automatic critical point dryer. The samples were then mounted on specimen mounts for scanning electron microscopes and gold coated using a Desk-II Cold sputter/ETCH Unit. SEM was performed using a JEOL JSM6360 LV equipment.

2.3. DNA extraction and ITS-2 amplification

The microalgae cells were harvested at the stationary growth phase by centrifugation (30 ml) and washed three times in bidistilled sterile water. The cell (ca. 200 mg) was stored at −20 °C, until use. For genomic DNA extraction, the Dellaporta [44] protocol was used with minor modifications. ITS-2 amplification was implemented using forward and reverse primers proposed by Van Hannen et al. [45]. ITS-2 assay was carried out with a 10 μl reaction mixture containing 1× PCR Buffer, 2 mM $MgCl_2$, 0.2 mM dNTPs, 1 mM primer, 1 U *Taq* DNA polymerase (Invitrogen) and 10 ng of DNA. PCR conditions included 1 cycle of 1 min at 94 °C for initial denaturation, followed by 35 cycles of 1 min at 94 °C, 1 min at 55 °C, 1.5 min at 72 °C, and finally 7 min at 72 °C. Amplicons were checked by electrophoresis on 1% agarose gel in 1× TAE buffer. The PCR products were sequenced in an ABI 377 DNA sequencer (Applied Biosystems, USA) using the BigDye terminator cycle sequencing ready reaction kit according to the manufacturer's instructions (Applied Biosystems, USA).

2.4. ITS-2 sequence analysis

ITS-2 sequence-structure analysis was carried out as follows. ITS2 Database phylogeny was used to extract the ITS-2 sequence with the "Annotation" tool [46,47]. The ITS-2 sequence was then used to "Predict" the secondary structure by homology modeling based on related taxa with a p-value < 10^{-16}. The modeled sequence-structures were used to perform a BLAST search on the ITS2 Database platform, and those that showed similarity were used as input in the 4SALE program [48] for the alignment of sequences and secondary structures by Clustal W. The 4SALE program was used to obtain the condensed-secondary structure and those for each strain under study, as well as the CBC matrix. CBCAnalyzer [49] was used to construct the CBC tree using NJPlot and the phylogenetic tree was visualized using the Dendroscope program [50]. The resulting DNA sequences were published in the NCBI databases under the specific accession number: DSRE-1, KF990552; DSRE-2, KF990551; SCRE-1, KF990554; SCRE-2, KF990555, and CORE-1, KF990553.

2.5. Fatty acid profiling: total lipid extraction and transesterification

The microalgae biomass was harvested by centrifugation at the end of the exponential growth phase, and then re-suspended in fresh TAP medium without NH_4Cl for 3 to 5 days, depending on the duration of the stationary growth phase of each strain. Before and after the N-limitation step, the biomass was harvested by centrifugation and freeze dried for extraction following a drying procedure based on the work of [51]. In order to achieve complete lipid extraction, dry cell pellets were crushed and extracted twice with 15 ml of chloroform/methanol 2:1 v/v. The solvent–biomass mixture was subsequently agitated by vortex and then at 150 rpm/38 °C/3 h. The supernatant was separated from the biomass and evaporated at 60 °C to obtain total lipid extraction. FAME (fatty acid methyl esters) were obtained using a modified protocol based on [52]. The lipid extract was dissolved in 300 μl heptane, 300 μl of sodium metoxide solution (0.35% w/w of crude extract), and 300 μl ethyl acetate were added. The reaction was performed under agitation at 45 °C for 90 min, and then the biodiesel was recovered from the upper phase. The fatty acid profile was determined by gas chromatography–mass spectrometry (GC–MS) analysis, carried out in an Agilent 6890 N gas chromatograph equipped with an Agilent 5975B mass selective detector. Compounds were profiled on a 30 m × 0.32 mm ID × 0.5 μm film Agilent DB-5 capillary column, carrier gas was He at 1.5 ml/min. Temperature conditions were 120 °C for 1 min, 15 °C/min ramp to 180 °C, 7 °C/min ramp to 230 °C and 10 °C/min ramp to 300 °C and held for 60 min. Ionization voltage was 70 eV and sample injection volume was 1 μl. GC analysis was carried out in a Perkin-Elmer Clarus gas chromatograph equipped with a FID detector. Compounds were profiled on a 15 m × 0.32 mm ID × 0.1 μm film Agilent DB5-HT capillary column. Carrier gas was N_2 at 3 ml/min. Temperature conditions were 50 °C for 1 min, 15 °C/min ramp to 180 °C, 7 °C/min ramp to 230 °C and 10 °C/min ramp to 300 °C and held for 10 min. Sample injection volume was 1 μl. The following standards were used for quantification: palmitic acid methyl ester, stearic acid methyl ester, and oleic acid methyl ester (Sigma-Aldrich).

All experiments were conducted in triplicate (n = 3). For statistical analysis, the MINITAB 16 (Minitab Inc., State College, PA, USA) software was employed. Significant differences among experiments were determined using the Fisher's least significant difference (LSD) procedure with $p \leq 0.05$.

Table 1
Pure component property data for the fatty esters present in biodiesels.

FAME	ρ @15 °C (kg/m^3)	b[a] (kg/m^3 K)	a[a] (kg/m^3)	CN	ν @40 °C[b] (mm^2/s)	HHV[c] (MJ/kg)	OSI[d] (h)
C14:0	871.3[e]	−0.7629	1091.1	66.2[f]	3.30	38.90	–
C16:0	869.4[e]	−0.7438	1083.7	74.5[f]	4.38	39.45	>24
C18:0	867.8[e]	−0.7209	1075.5	86.9[f]	5.85	40.07	>24
C18:1	877.7[g]	−0.7236	1086.2	56.0[h]	4.51	39.91	2.79
C18:2	889.9[g]	−0.7294	1100.0	41.7[h]	3.65	39.70	0.94

[a] Parameters of Eq. (2) for calculation of density as a function of temperature.
[b] [10]. Method: ASTM D445.
[c] [56]. Method: modification of ASTM D240 and D2015.
[d] [9]. Method: AOCS Cd12b-92 or EN 14112.
[e] Calculated using Eq. (2) reported by Pratas [55].
[f] [53]. Method: ASTM D613.
[g] [55].
[h] [54]. Method: ASTM D613.

Table 2
Compensatory base change of strains under study: SCRE-1, SCRE-2, CORE-1, DSRE-1 and DSRE-2.

	DSRE-1_ KF990552	SCRE-2_ KF990555	300713803_ Coelastrum_ sphaericum	159135731_ Desmodesmus_ pleiomorphus	40288343_ Desmodesmus_ multivariabilis_ var._turskensis	40288336_ Desmodesmus_ multivariabilis_ var._turskensis	6625532_ Scenedesmus_ obliquus	46241854_ Scenedesmus_ bajacalifornicus
6625508_Scenedesmus_acutus	7	0	3	6	7	7	0	0
SCRE-1_KF990554	7	0	3	6	7	7	0	0
4972014_Scenedesmus_acuminatus	7	0	3	7	8	8	1	0
89515343_Desmodesmus_multivariabilis_ var._turskensis	0	7	4	0	0	0	7	6
CORE-1_KF990553	5	1	1	5	6	6	2	1
56122680_Desmodesmus_pleiomorphus	0	6	4	0	0	0	6	5
40288338_Desmodesmus_multivariabilis	0	7	4	0	0	0	7	6
6625510_Scenedesmus_acuminatus	7	0	3	7	8	8	1	0
300713799_Coelastrum_proboscideum_ var._dilatatum	4	3	0	4	4	4	3	2
300713803_Coelastrum_sphaericum	4	3	0	4	4	4	3	2
6625532_Scenedesmus_obliquus	7	0	3	6	7	7	0	0
6625508_Scenedesmus_acutus	7	0	3	6	7	7	0	0
89515370_Desmodesmus_sp._Mary6/3T-2d	3	5	6	2	3	3	5	4
40288335_Desmodesmus_pleiomorphus_ var._kantonensis	0	7	4	0	0	0	7	6
169798019_Desmodesmus_sp._MAT-2008c	1	7	5	1	1	1	7	6
159135712_Desmodesmus_sp._EH21	2	6	6	2	2	2	6	5
300713800_Coelastrum_proboscideum_ var._gracile	4	3	0	4	4	4	3	2
300713799_Coelastrum_proboscideum_ var._dilatatum	4	3	0	4	4	4	3	2
40288331_Desmodesmus_multivariabilis	0	7	4	0	0	0	7	6

2.6. Estimation of biodiesel properties

Estimation of biodiesel properties was performed by using the FAME profiles determined for the extracted microalgae lipids before and after the N-limitation step, in conjunction with property data for pure fatty esters gathered from the literature and summarized in Table 1. This information was used in combination with a suitable mixing rule, and for some properties (e.g., cold flow plugging point) selected correlations taken from the literature were applied. The following seven main biodiesel properties described in Section 1 were estimated: density at 15 °C and 40 °C (ρ), cetane number (CN), kinematic viscosity at 40 °C (ν), higher heating value (HHV), iodine value (IV), cold flow plugging point (CFPP), and oxidative stability (OSI).

The simple Kay's mixing rule given by Eq. (1) was used to estimate ρ, CN, ν, HHV, and IV, starting from the properties of individual fatty esters present in a given biodiesel. Estimation of CFPP and OSI will be described below. As stated above, the use of Eq. (1) is justified for predicting biodiesel properties, considering that they are simple mixtures constituted by less than 10 single compounds of the same family, thus having similar physicochemical properties.

$$f_B = \sum_{i=1}^{n} x_i \cdot f_i. \tag{1}$$

In Eq. (1), f was replaced in each case by ρ, CN, $ln\ \nu$, HHV or IV, depending on the property or parameter to be calculated. n is the number of fatty esters in the mixture and x is the weight fraction. Subscript i refers to the individual *ith* fatty ester and subscript B refers to the mixture of esters or biodiesel.

The density of some individual fatty esters at 15 °C was calculated based on Pratas et al. [55]. These authors reported their experimentally determined density data (Table 1), as well as the correlation given by Eq. (2), developed to calculate the density of individual fatty esters as a function of temperature.

$$\rho\left[\frac{\mathrm{kg}}{\mathrm{m}^3}\right] = b * T[K] + a. \tag{2}$$

With respect to the density calculation, it is important to state that among the fatty esters present in the biodiesels studied in this work (Table 2), only methyl oleate (C18:1) and methyl linoleate (C18:2) are liquid at 15 °C, and their density values were taken from Pratas et al. [55]. For the rest of the fatty esters, densities at this temperature were therefore estimated by using Eq. (2), developed by the same authors to calculate the density of individual FAMEs as a function of temperature. Values of parameters a and b in this equation are also shown in Table 2

For biodiesel IV estimation, the required IV of individual fatty esters was calculated with the use of Eq. (3), by assuming full iodization, as described by Knothe [57]:

$$IV_i = 100 \cdot \frac{253.81 \cdot db_i}{MW_i}. \tag{3}$$

In Eq. (3), db_i and MW_i are the number of double bonds and the molecular weight of the fatty ester i respectively, while 253.81 is the atomic weight of two iodine atoms that are theoretically added to one double bond.

On the other hand, estimation of CFPP was performed using Eqs. (4) and (5), as proposed by Ramos et al. [34]. The first step was to estimate what those authors called the Long Chain Saturated Factor (LCSF) by using Eq. (4) and then substitute the value of this parameter into Eq. (5).

$$\mathrm{LCSF} = 0.1 \cdot \mathrm{C16} + 0.5 \cdot \mathrm{C18} + 1 \cdot \mathrm{C20} + 1.5 \cdot \mathrm{C22} + 2 \cdot \mathrm{C24} \tag{4}$$

$$\mathrm{CFPP} = 3.1417 \cdot \mathrm{LCSF} - 16.477. \tag{5}$$

In Eq. (4), C16, C18, etc. are the weight percentages of the species having saturated chains with 16, 18, etc. carbon atoms. In order to calculate the CFPP of biodiesels in this work, only the first and second terms on the right-hand side of Eq. (4) were taken into account, since fatty esters with more than 18 carbons in the hydrocarbon chain were absent.

The estimation of oxidative stability (OSI) was performed according to Park et al. [58]. These authors proposed the correlation given by

300713800_ Coelastrum_ proboscideum_ var._gracile	6625508_ Scenedesmus_ acutus	4972014_ Scenedesmus_ acuminatus	89515371_ Desmodesmus_sp._ Tow10/11 T-2 W	89515367_ Desmodesmus_ asymmetricus	DSRE-2_ KF990551	6625532_ Scenedesmus_ obliquus	89515395_ Desmodesmus_ asymmetricus	89515394_ Desmodesmus_ asymmetricus	40288333_ Desmodesmus_ pleiomorphus
3	0	1	5	5	4	0	6	7	6
3	0	0	5	4	4	0	5	5	6
3	1	0	5	4	4	1	5	5	7
4	7	8	3	3	0	7	3	3	0
1	2	2	4	4	3	2	5	5	5
4	6	7	2	2	0	6	3	3	0
4	7	8	3	3	0	7	3	3	0
3	1	0	5	4	4	1	5	5	7
0	3	3	6	5	3	3	5	5	4
0	3	3	6	5	3	3	5	5	4
3	0	1	5	5	4	0	6	7	6
3	0	1	5	5	4	0	6	7	6
6	5	5	0	2	0	5	2	1	2
4	7	8	3	3	0	7	4	4	0
5	7	7	1	2	0	7	2	2	1
6	6	6	0	1	0	6	1	1	2
0	3	3	6	5	3	3	5	5	4
0	3	3	6	5	3	3	5	5	4
4	7	8	3	3	0	7	3	3	0

Eq. (6), in which *X* is the weight percentage of methyl oleate plus methyl linoleate, and *Y* is the oxidation stability in hours.

$$Y = 117.9295/X + 2.5905. \quad (6)$$

2.7. Assessment of accuracy in the estimation of biodiesel properties

The accuracy of the predictions of biodiesel quality was estimated in the following manner: for each quality parameter, the value of the property for different biodiesels and their corresponding fatty ester profiles were gathered from the literature. With this information, the value of the property was calculated using the corresponding correlation and/or mixing rule applied in this work. Subsequently, the average absolute deviation (AAD) between the experimental and estimated values was calculated by using Eq. (7), in which N_p is the number of data points considered for a given data set and *P* is the property of interest. More details on these procedures are outside of the scope of the present work and will be provided in a personal communication.

$$AAD(\%) = \frac{1}{N_p} \cdot \sum_{i=1}^{N_p} \left| \frac{100 \cdot \left(P_{i,exp} - P_{i,\ calc}\right)}{P_{i,exp}} \right|. \quad (7)$$

3. Results and discussion

3.1. Classification of strains under study

3.1.1. Cell surface characterization with scanning electron microscopy (SEM)

Ultrastructural cell wall features are essential for supporting the placement of the different strains into the *Scenedesmus* and *Desmodesmus* subgenera. The subgenus *Scenedesmus* includes all spineless species with obtuse cell poles and without cell wall structures on the sporopollenin cell wall [59]. On the other hand, subgenus *Desmodesmus* is characterized by cell wall structures in the form of granulation spines, warts, ribs and other ornamentations at the outer cell wall layer [60,40].

The micrographs taken with SEM were focused on descriptions of the size and shape of the cells and the presence of ornamentation of the cell wall to determine whether each strain belongs to the mentioned species. DSRE-1 and SCRE-1, both acquired from CICESE, showed different morphology. Strain DSRE-1 showed coenobia of two and four cells (Fig. 1A). The oval shaped-cell, 3.55–4.32 μm in length and 7.43–8.74 μm in width, showed two rib-shaped rows of tiny spines equidistant from pole to pole. The outer cells present two short, thick spines at their base (462 nm × 384 nm). On the cell surface we can observe granulations distributed in rows from pole to pole, and some scattered on the surface forming small clusters on the top of each cell. The presence of microtubules (47.2–50.7 nm) is clear over each cell, forming a network (90.9 nm × 114 nm) which linearly interconnects each of the outer and inner cells. According to this description, this strain belongs to the subgenus *Desmodesmus*, although it had been registered as belonging to the subgenus *Scenedesmus*.

The SCRE-1 strains showed coenobia of four cells. It is single-celled, 3.31–5.69 μm in length and 4.84–10.5 μm in width (Fig. 1B). The elongate-ovoid cell in lateral position showed a truncated protuberance which was slightly elongated on one pole. On the cell surface, scattered granulations were observed as well as a rib extending from the pole. Strains of *Scenedesmus*, such as *S. obliquus*, have previously been mislabeled as *Scenedesmus acutus* based on morphological characteristics [41]. This *S. obliquus*-like strain showed morphologic traits indicating that it belongs to the subgenus *Scenedesmus*.

The related strain SCRE-2 was predominantly single-celled, 5.18–6.43 μm in length and 7.50–9.49 μm in width (Fig. 1C). The lemon-shaped cell showed short truncated poles. The cell surface was almost smooth with irregular transverse lines, apparently dehydrated. According to the description, this strain is similar to *S. obliquus* species.

Meanwhile, the strain CORE-1 showed isolated cells (coelastroides) of 4.88–7.12 μm in height and 7.52–9.90 μm in width (Fig. 1D). The lemon-shaped cell showed truncated ovoid poles. The cell surface is slightly rough from pole to pole and lateral striations are thinly spaced

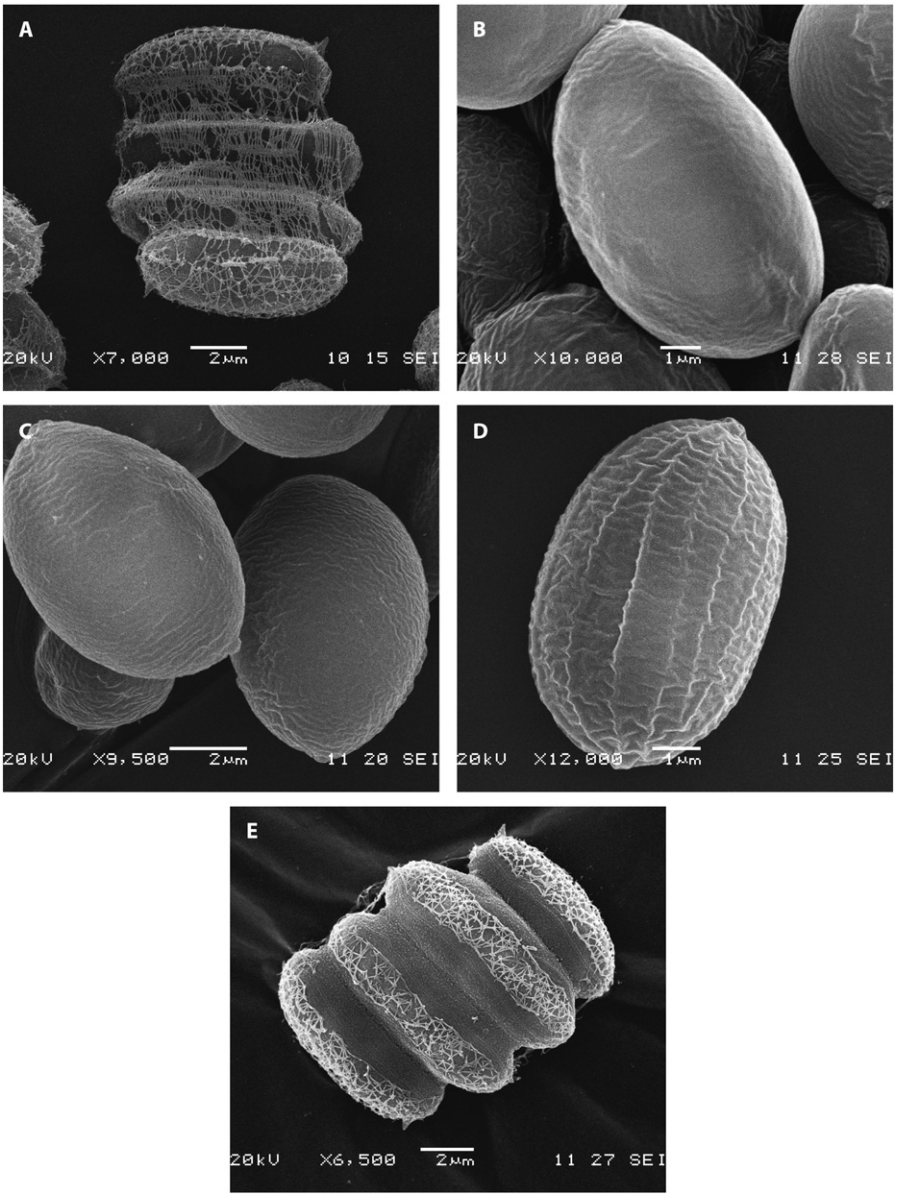

Fig. 1. Scanning electron micrographs of the cells of microalgal strains growing in TAP medium. A: SCRE-1; B: SCRE-2; C: CORE-1; D: DSRE-2 and E: DSRE-1.

between the vertical striations, giving it a slightly rough appearance like the surface of a peanut.

Isolated cultured cells were predominantly observed. However, mother cells were observed indicating asexual reproduction by autospores. This strain showed a cell wall with similar ornamentations to some collected by Lewis and Flechtner [61] from desert microbiotic crust communities in western North America. Those strains, as with strain CORE-1 in this study, showed fine filaments connecting cells pole to pole, and a lack of spines, warts, and other wall ornamentation. This has been observed in some documented isolates, such as *Scenedesmus* (*Dactylococcus*) *dissociatus* and *S. obliquus*.

Finally, *D. spinosus*, labeled DSRE-2 (Fig. 1E), showed coenobia of two to four cells joined by the cell wall. The cell of 3.11 μm in length and 8.83 μm in width possesses granulations on its surface and two rows of rib-shaped granules equidistant from pole to pole on each of the cells. On each of the outer cells, the presence of short, thick spines is evident, as well as a network of microtubules on the upper surface of the outer cells and at opposite ends of each of the internal cells. The ornamentations of this strain confirmed that it belongs to the subgenus *Desmodesmus*, although the identity of the species was not confirmed by its morphologic traits.

3.1.2. ITS-2 analysis

The primers used successfully amplified the ITS-2 region from DNA of the SCRE-1, SCRE-2, CORE-1, DSRE-1 and DSRE-2 strains under study. The amplicon average was 391 pb. This sequence was submitted to the ITS2 Database to delete the flanking regions of the ITS2 (5.8S and 28S) before predicting the structure with the Annotation tool. After prediction of each sequence, BLAST analysis was performed on ITS2 sequence-structure.

The sequence and secondary structure analysis of ITS-2 clearly indicated a good separation of the investigated strains into four groups (Fig. 2). Group I was subdivided between SCRE-1 and SCRE-2 strains. Strain SCRE-1 registered as *S. obliquus* was clustered with accessions registered as *Scenedesmus acuminatus*. Strain SCRE-2 registered as *S. incrassatulus* was clustered with accessions registered as *S. obliquus* and *S. acutus*. The SCRE-1 and SCRE-2 strains showed smooth cell walls without ornaments, and were spineless with obtuse cell poles. This

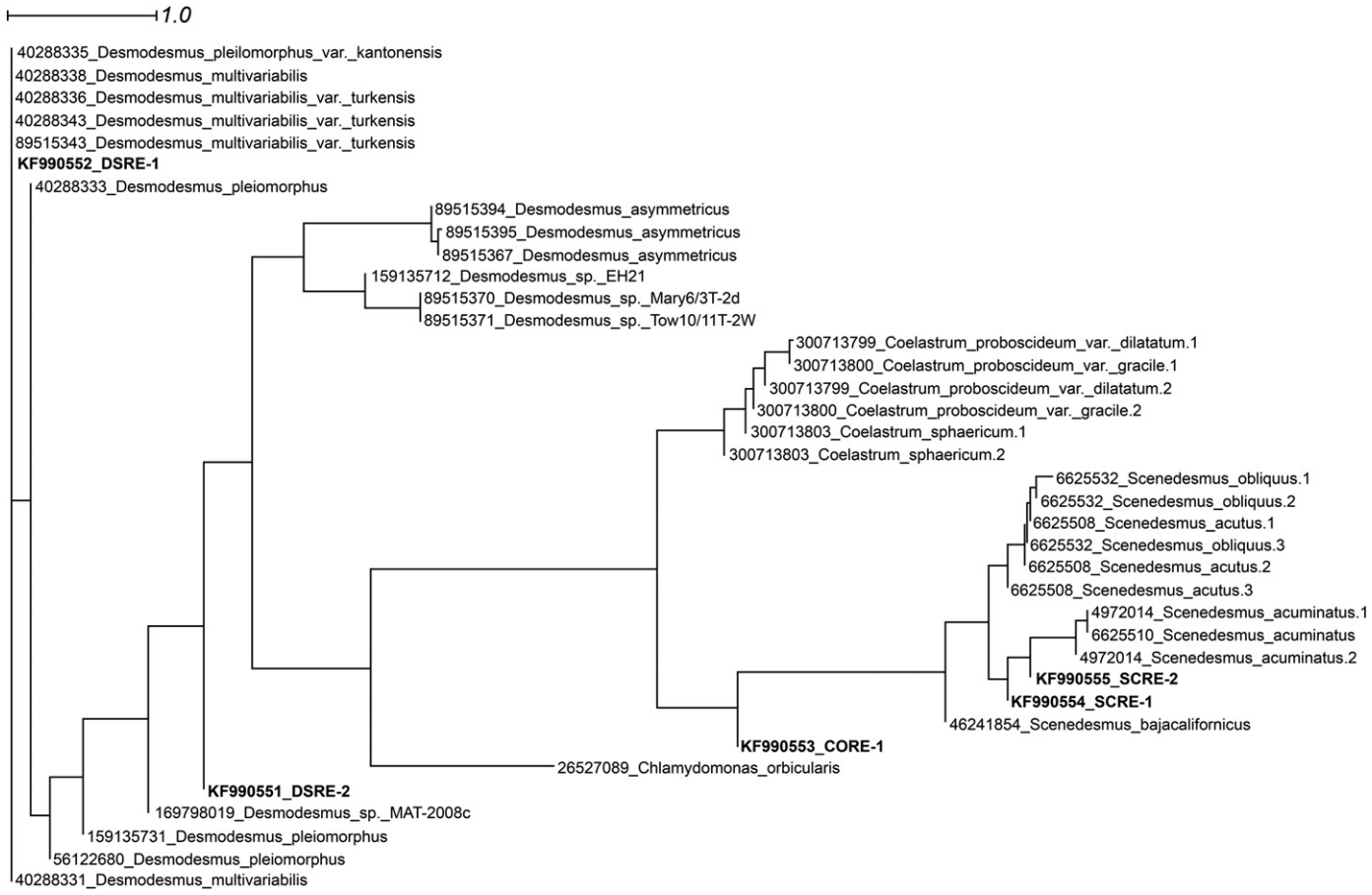

Fig. 2. CBC tree of five fresh water microalgae, constructed from CBC matrix using NJPlot as implemented in CBCAnalyzer.

means that it should be classified as *Scenedesmus* sp., whose cells are spineless with obtuse cell poles and do not have ornaments or structures on the cell wall [62].

Strain CORE-1 was clustered between *Scenedesmus* and *Coelastrum* species, exhibiting a shorter genetic distance with respect to *Coelastrum* species than the other one (Fig. 2). The identity of the CORE-1 strain as *Coelastrum* species was supported by morphologic characterization, since it showed a cell wall with a rough appearance, contrary to *Scenedesmus* strains. The clustering of CORE-1 and *Coelastrum* accessions near to SCRE-1, SCRE-2 and *Scenedesmus* accessions is explained by the fact that spherical coenobia of *Coelastrum* and allied species are phylogenetically closely related to the flat coenobia with cells arranged in one or two rows of *Scenedesmus* relatives [63].

On the other hand, strains DSRE-1 and DSRE-2 were clustered as *Desmodesmus* species. This is reasonable because both strains showed ornaments on the cell wall. Strain DSRE-1, previously registered by the Culture Collection at CICESE as *Scenedesmus* strain, was clustered close to *Desmodesmus multivaribilis* and *Desmodesmus pleiomorphus* accessions. This clustering is reasonable, because *D. multivaribilis* shows the presence of microtubules forming a network (Fig. 1A and E). The DSRE-2 strain previously registered as *D. spinosus* was clustered with *Desmodesmus* sp. and *Desmodesmus asymmetricus*. The DSRE-2 strain should therefore be classified as belonging to *Desmodesmus* sp.

Compensatory base changes' (CBCs) matrix results are discussed here and shown in Table 2. There is no CBC between strain SCRE-1 with respect to *S. obliquus*, *S. acuminatus* and *S. bajacalifornicus* accessions. This suggests that strain SCRE-1 identity falls into all of them with a probability of 0.76. The same applies to strain SCRE-2. Consequently, we propose that SCRE-1 and SCRE-2 strains should be placed within *Scenedesmus* sp. until a complete taxonomic study is carried out. In this regard, there is a good basis for applying the criteria of Müller [64]; a lack of a CBC in the ITS2 secondary structure is not necessarily a sign that the organisms belong to the same species.

On the other hand, there is at least one CBC between strain CORE-1 with respect to all accessions and strains under study. This result indicates that strain CORE-1 belongs to a different species. This separation is indicative of total incapability of intercrossing with the rest of the strains tested. It could be considered to belong to the *Coelastrum* genus.

With respect to the other strains, there is no CBC between strain DSRE-1 and *D. multivariabilis* and *D. pleiomorphus*. This indicates that strain DSRE-1 could be strongly considered to belong to the subgenus *Desmodesmus*. Similar results were obtained for strain DSRE-2, where there is no CBC between this and all other *Desmodesmus* accessions. This strongly confirms that strain DSRE-2 belongs to this subgenus. A complete taxonomic study will be carried out for species assignment to DSRE-1 and DSRE-2 strains. We therefore recommend that both strains be classified as *Desmodesmus* sp. strains.

3.2. Growth of microalgae strains

All identified strains showed a lag phase of 2 or 4 days before they began exponential growth for approximately 3 more days (Fig. 3). Strains belonging to *Scenedesmus* species showed similar growth patterns. SCRE-1 cell concentration at the end of exponential growth (day 5 of culture) was not significantly different from SCRE-2. Despite this, SCRE-1 cell number was slightly higher than SCRE-2 between days 6 to 9 and the decay in cell concentration was more evident with SCRE-1. CORE-1 reached its highest growth at day 5, producing 63% of the cell concentration produced by SCRE-1 and SCRE-2. The cell number remained constant until the end of culture.

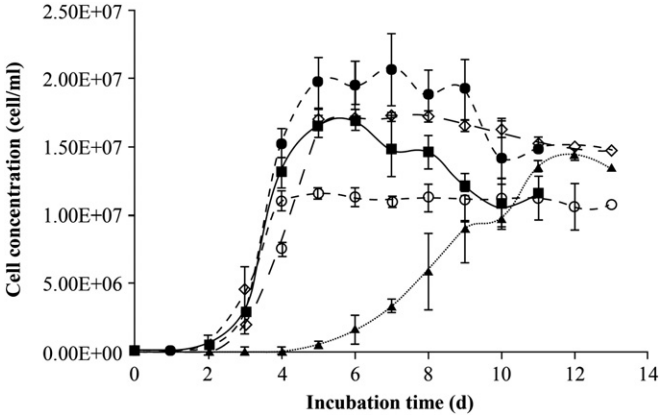

Fig. 3. Microalgae growth curves. SCRE-1 (●), SCRE-2 (◊), CORE-1 (○) DSRE-1 (■) and DSRE-2 (▲).

Different strains of *Desmodesmus* species showed different growth patterns. DSRE-1 reached the highest cell number at day 6, but this was only maintained for 2 days before the decay phase. DSRE-2 showed a longer adaptation (lag phase) to culture conditions, but was able to reach a similar cell concentration to *Scenedesmus* species at the end of its exponential growth (day 12 of culture).

Growth curves indicate that in the case of *Scenedesmus* subgenus strains SCRE-1 and SCRE-2, and even CORE-1 of *Coelastrum* genus, the stationary phase was attained at day 5 of culture in complete TAP medium. During this phase, the cells redirect their biosynthetic pathways to triacylglycerol synthesis [65], and this time was therefore used to begin the N-limitation step for 5 more days.

The N-limitation step on *Desmodesmus* strains was induced at day 5 and maintained for 5 more days for DSRE-1. Although DSRE-2 showed the longest growth (11 days) in complete TAP medium and N-limitation was carried out for only 3 more days, the resulting lipid profile showed better properties as a biodiesel feedstock than the other strains.

3.3. Biomass and volumetric lipid productivity

Biomass productivity is an important factor for assessing the potential of microalgae for biofuel production [14]. N-limitation promoted an increase in biomass ranging from 1.7 to 3.5 times in all strains under study. The highest biomass dry weight at the end of the N-limitation phase was obtained from strain CORE-1, followed by DSRE-1 and DSRE-2 (Fig. 4). Although DSRE-2 presented slower growth in complete TAP medium, it managed to reach a similar biomass yield to SCRE-2 and DSRE-1.

Lipid accumulation after N-limitation was found to follow the same pattern as dry biomass weight (Fig. 4) and was particularly enhanced by nitrate limitation (between 2.5 and 4.1 times greater). Strain CORE-1 produced a higher lipid productivity (69.6 mg/l/d) followed by strains SCRE-1 and DSRE-1 with a lipid productivity of 52.9 and 48.9 mg/l/d respectively. The lowest lipid production was obtained with SCRE-2 and DSRE-2 strains, with 36 and 29.3 mg/l/d respectively. These results prove that the strains evaluated in this work responded to N-limitation, reaching a higher yield of biomass and lipids.

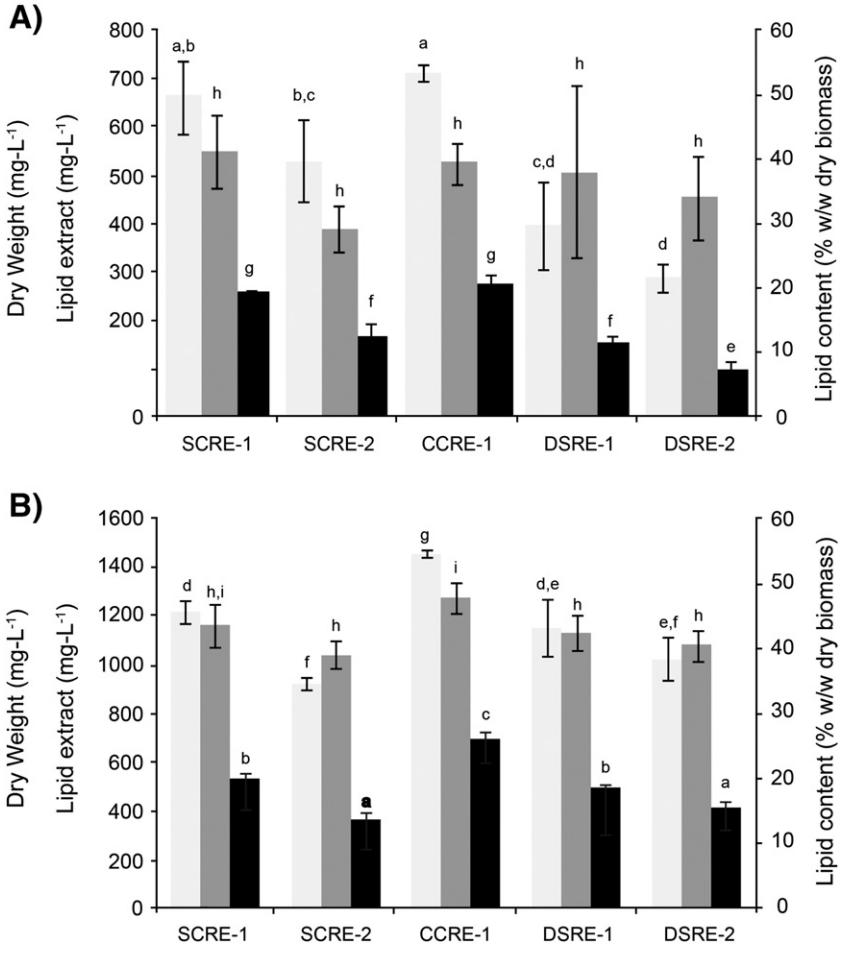

Fig. 4. Dry biomass weight (light gray bars), lipid extract (dark bars) and lipid content (dark gray bars) of microalgae cultures before and after N-limitation (panels A and B respectively). Different letters indicate statistically significant differences.

Lipid content was similar for all strains (39–44%, w/w), with the exception of CORE-1, whose lipid content was the highest (48%, w/w) and significantly different from the rest of the strains (Fig. 4). This is the highest lipid content reported for *Coelastrum microporum* (25.99%, w/w) [17], although similar to those reported for *S. obliquus* (SAG 276-3) after nitrate limitation (43%, w/w) [24] and *Desmodesmus* sp. (WC08) with 31.30% w/w [19]. Although the results indicated that all studied strains increased their biomass production and lipid accumulation after N-limitation stress under the conditions tested in this work, differences were found in fatty acid composition.

3.4. Transesterification

The main FAME (fatty acid methyl esters) produced by the strains tested in this work before and after N-limitation were C14:0, C16:0, C18:0, C18:1 and C18:2 (Table 2). Nearly 90% of the fatty acid esters identified after N-limitation were due to the presence of C16:0 and C18:1 for all five strains evaluated. Unidentified compounds detected before and after N-limitation accounted for less than 6% of total lipid extract.

FAME profiles differed before and after N-limitation for most of the microalgae strains. Percentages of C16:0, C18:0 and C18:1 increased after N-limitation, indicating that the FAME profile before and after N-limitation depended on microalgae species. For example, DSRE-1 and DSRE-2 from *Desmodesmus* subgenera showed a higher percentage of C18:1 than SCRE-1 and SCRE-2 from *Scenedesmus* subgenera. It has been reported that fatty acid composition depends on the physiological potential of each strain [13].

These results are similar to those obtained by Pan et al. [66] for DSRE-2, which showed C18:1 as the most abundant fatty acid, followed by C16:0. A high C18:1 content is desirable for biodiesel production given the high quality fuel properties exhibited by this fatty ester (Table 1).

Under N-limitation, the microalgae fatty acids are mainly composed of C16:0 and C18:1 (around 90%), which are the fatty acids most commonly synthesized by *Chlorophyceae* [65] and present in biodiesel as methyl esters [9,21]. The percentages of C16:0 and C18:1 obtained with the strains characterized in this work were higher after N-limitation than those reported by Kaur et al. [22] for six freshwater microalgae belonging to *Scenedesmus* and *Desmodesmus* genera without N-limitation. Similar results were obtained by Abou-Shanab et al. [67] for five strains of *S. obliquus* and *Chlamydomonas* genera without N-limitation. This proved that nitrogen-limited microalgae cultures could reach a higher lipid yield than nitrogen-replete cultures.

Values obtained after nitrogen limitation are indicated in parenthesis.

3.5. Estimation of biodiesel properties

Seven main fuel properties were calculated according to Section 2.6 for biodiesels obtained before and after N-limitation of the five strains. Predicted properties are summarized in Table 4, in which the corresponding U.S. and European biodiesel specifications are also shown.

3.5.1. Density

The estimated density at 15 °C of the five biodiesels before and after N-limitation is around 880 kg/m^3 and falls within the limits established in EN 14214. The U.S. biodiesel standard (ASTM D6751), meanwhile, does not specify limits for this property. It is important to note, however, that some biodiesels in this work have low percentages of the esters that are liquid at 15 °C (C18:1 and C18:2). Among them, SCRE-1 showed the lowest concentrations of these, containing 6.97 wt.% of C18:1 and 0 wt.% of C18:2, as shown in Table 2. Therefore, it is likely that SCRE-1 is not liquid at 15 °C. However, it was decided to include it in Table 4 with the rest of the estimated densities for comparison purposes.

3.5.2. Cetane number

The results for the prediction of this property indicate that all biodiesels from the strains under study exhibit CN values well above the more stringent minimum limit of 51 established in the European biodiesel standard (Table 4). For the SCRE-1, SCRE-2 and CORE-1 strains, lower CN values were obtained prior to N-limitation. This is explained by the higher concentration of unsaturated esters in these biodiesels, because unsaturated species cause lower CN values (Table 1). For DSRE-2 strain, a higher concentration of unsaturated species was obtained after N-limitation, resulting in a lower CN than before limitation.

3.5.3. Kinematic viscosity

As shown in Table 4, kinematic viscosity for all biodiesels (before and after N-limitation) meets both the American and the European biodiesel standards. It can be observed that all kinematic viscosities calculated for biodiesels after N-limitation are slightly higher than the viscosities before limitation. In the case of SCRE-1, SCRE-2 and CORE-1 strains, higher viscosities are explained due to the higher concentrations of saturated FAMEs (Table 3), because saturated esters have higher kinematic viscosities than unsaturated ones, as can be seen in Table 1. On the other hand, biodiesels from DSRE-1 and DSRE-2 strains also presented higher viscosities after the limitation step, despite having lower concentrations of saturated FAMEs. This is explained by the high concentration of shorter species (C14:0 and C16:0), because kinematic viscosities for individual FAMEs are lower for species with shorter hydrocarbon chains (Table 1).

3.5.4. Heat of combustion

As occurs with CN and kinematic viscosity, HHV increases with increasing chain length and decreases with the presence of double bonds in the esters (Table 1). However, in this case the increase in the value of the property from one fatty ester to another is extremely small, and the reported values for the FAMEs under consideration range from 38.9 MJ/kg for C14:0 to 40.07 MJ/kg for C18:0. For this reason, the HHV for all biodiesels (before and after N-limitation) is 40 MJ/kg, which is, in fact, the average value usually reported for different types of biodiesel fuels.

Table 3
Composition of biodiesel from five microalgae strains at the end of exponential growth.

	Biodiesel composition (wt.%)				
	SCRE-1	SCRE-2	CORE-1	DSRE-1	DSRE-2
Methyl myristate (C14:0)	4.31 (2.94)	8.28 (2.73)	2.94 (2.52)	7.68 (1.13)	10.38 (1.23)
Methyl palmitate (C16:0)	37.04 (80.84)	53.46 (66.77)	28.87 (53.87)	45.16 (36.95)	42.48 (26.86)
Methyl stearate (C18:0)	1.65 (9.26)	3.01 (10.37)	1.22 (10.97)	2.25 (3.60)	1.41 (4.62)
Methyl oleate (C18:1)	27.88 (6.97)	35.25 (20.13)	31.28 (32.64)	20.74 (44.16)	35.29 (59.77)
Methyl linoleate (C18:2)	29.12 (0.00)	0.00 (0.00)	35.69 (14.15)	24.17 (7.51)	10.45 (0.00)
Saturated-FAME	43.00 (93.04)	64.75 (79.87)	33.03 (67.36)	55.09 (41.68)	54.27 (32.71)

3.5.5. Iodine value

As shown in Table 4, the highest IV among the five biodiesels after N-limitation corresponds to DSRE-2, at 64 g I/100 g biodiesel. Meanwhile, the highest IV among the biodiesels obtained before N-limitation corresponds to CORE-1, with an IV of 88 g I/100 g biodiesel. Thus, all the biodiesels are well below the maximum limit of 120 g I/100 g biodiesel prescribed by the EN 14214 standard. It should be noted that, in each case, the highest IV corresponds to biodiesels with the highest unsaturated fatty ester content (Table 1).

3.5.6. Cold filter plugging point

The CFPP value increases proportionally to the concentration of saturated fatty esters in a given biodiesel, and this increase is more pronounced for larger fatty esters (see Eqs. (4) and (5)). As such, for the group of biodiesels after N-limitation, the lowest (−1 °C) and the highest (23 °C) CFPP were obtained for DSRE-2 and SCRE-1 biodiesels, which showed the lowest (32.71 wt.%) and highest (93.04 wt.%) concentrations of saturated FAMEs respectively (Table 3). This parameter was poor for SCRE-1, SCRE-2 and CORE-1 biodiesels, with values greater than or equal to 18 °C.

All biodiesels before N-limitation exhibited conveniently low CFPP values that ranged from −1 to 5 °C. These lower CFPPs were obtained due to lower concentrations of saturated FAMEs in these biodiesels. The highest CFPP (5 °C) was obtained for SCRE-2, which is the biodiesel with the highest concentration (64.75 wt.%) of saturated FAMEs within this group (Table 3). Although this is a considerably high concentration of saturated species, the absence of the FAME with the highest impact on CFPP (C18:2) among the considered FAMEs allows the CFPP to maintain in an acceptable value.

3.5.7. Oxidative stability

Contrary to what occurs in the case of the CFPP parameter, oxidative stability is highly favored by the presence of high concentrations of saturated fatty esters. Table 4 shows that all biodiesels (before and after N-limitation) meet the American standard, which establishes a minimum of 3 h for this parameter. In the case of biodiesels obtained after N-limitation, only DSRE-1 and DSRE-2 biodiesels are below the minimum limit of 6 h set by the European standard. As can be seen in Table 3, these biodiesels presented the lowest concentrations of unsaturated fatty esters. On the other hand, in the case of biodiesels obtained before the limitation step, only SCRE-2 biodiesel reaches the minimum limit established in the European standard, and is the biodiesel with the highest concentration of saturated fatty esters (Table 3).

3.6. Accuracy of the property estimation methods

According to the procedure described in Section 2.7, the AAD values summarized in Table 5 were obtained for the seven methods for predicting biodiesel quality parameters.

Table 5
AAD calculated for the applied property estimation methods.

Property	Number of biodiesels	Total number of FAMEs	AAD (%)
ρ	11	14	0.0025
ν	11	12	0.47
CN	11	8	5.0
HHV	10	13	0.45
IV	10	6	8.9
CFPP	10	14	17
OSI	21[a]	8	8.9

[a] Biodiesel blends.

According to these results, prediction of density, kinematic viscosity and HHV of a given biodiesel can be performed with high accuracy by using the methods applied in this work. On the other hand, the error in predicting CN, OSI and IV can be considered moderate, while the deviation in the prediction of CFPP is high, meaning that more reliable estimation procedures need to be developed for this property.

4. Conclusions

Detailed characterization, including morphological, genetic and biotechnological analysis, applied to these five genetically related microalgae allow us to clearly state that these strains belong to the family Scenedesmaceae. In particular, ITS-2 sequence and secondary structure analysis permitted a genetic separation between strains SCRE-1 and SCRE-2 belonging to *Scenedesmus* subgenus, and DSRE-1 and DSRE-2 belonging to *Desmodesmus* subgenus. Moreover, this genetic approach made it possible to classify the strain CORE-1, formerly classified as member to *Scenedesmus* subgenus, as probably belonging to the genus *Coelastrum*, which shares phylogenetic relations with Scenedesmaceae family. However, more research must be conducted in all cases to reliably clarify the identity of these microalgae. In this regard, physiological analysis will be of particular importance.

All biodiesels (before and after N-limitation) showed quite good values for the density (ρ), cetane number (CN), kinematic viscosity (ν), higher heating value (HHV) and iodine value (IV) properties, and they complied with the American and European biodiesel standards. Thus, the major differences in the quality of the obtained biodiesels are focused on the cold filter plugging point (CFPP) and oxidative stability (OSI) property values.

All biodiesels before N-limitation exhibited satisfactory CFPP values (−1 to 5 °C) and all met the American standard for OSI, but only SCRE-2 biodiesel complied with this parameter according to the European standard. This means that SCRE-2 (before N-limitation) was the only biodiesel that met all estimated parameters of the more stringent European standard while showing good cold flow properties (CFPP = 5).

Table 4
Predicted biodiesel properties and specifications in the U.S. and European standards. Values obtained after and before (in parenthesis) N-limitation.

Property (units)	SCRE-1	SCRE-2	CORE-1	DSRE-1	DSRE-2	ASTM D6751	EN 14214
ρ @15 °C (kg/m^3)	883	880	883	882	881		860–900
	(880)	(880)	(880)	(881)	(880)		
CN	60	68	57	62	64	47 min	51 min
	(74)	(72)	(70)	(62)	(61)		
ν @40 °C (mm^2/s)	4.2	4.4	4.1	4.2	4.2	1.9–6.0	3.5–5.0
	(4.5)	(4.5)	(4.5)	(4.4)	(4.4)		
HHV (MJ/kg)	(40)	(40)	(40)	(40)	(40)		
	40	40	40	40	40		
CFPP (°C)	−2	5	−5	1	−1		
	(23)	(21)	(18)	(1)	(−1)		
IV (g I/100 g biodiesel)	74	30	88	59	48		120 max
	(6)	(17)	(28)	(62)	(64)		
OSI (h)	5	6	4	5	5	3 min	6 min
	(20)	(8)	(6)	(5)	(4)		

In the case of biodiesels after N-limitation, DSRE-1 and DSRE-2 biodiesels showed good cold flow properties (1 and −1 °C, respectively), and their OSI values met the limits established in the American biodiesel standard, but not the European one. While SCRE-1, SCRE-2 and CORE-1 biodiesels did meet the OSI parameter according to the European standard, they showed poor cold flow properties (CFPP ≥ 18 °C).

Moreover, it was found that ρ, ν and HHV can be predicted with high accuracy by using the methods applied in this work (AADs ≤ 0.47%). On the other hand, the error in predicting CN, IV and OSI can be considered moderate (5% ≤ AAD ≤ 8.9%), and the deviation in the prediction of CFPP was high (AAD = 17%). The development of more reliable correlations for the estimation of OSI, IV and CFPP is necessary to improve the accuracy in the prediction of biodiesel quality.

Acknowledgments

The authors gratefully acknowledge the financial support granted by the Consejo Nacional de Ciencia y Tecnología (CONACyT, Mexico) project Nos. 149135 and 166371. We acknowledge Paola Marfil Lara for edition of figures.

References

[1] B.E. Rittmann, Opportunities for renewable bioenergy using microorganisms, Biotechnol. Bioeng. 100 (2008) 203–212.
[2] M.J. Groom, E.M. Gray, P.A. Townsend, Biofuels and biodiversity: principles for creating better policies for biofuel production, Conserv. Biol. 22 (2008) 602–609.
[3] M.B. Johnson, Z. Wen, Production of biodiesel fuel from the microalga *Schizochytrium limacinum* by direct transesterification of algal biomass, Energy Fuel 23 (2009) 5179–5183.
[4] F.B. Metting Jr., Biodiversity and application of microalgae, J. Ind. Microbiol. 17 (1996) 477–489.
[5] P. Spolaore, C. Joannis-Cassan, E. Duran, A. Isambert, Commercial applications of microalgae, J. Biosci. Bioeng. 101 (2006) 87–96.
[6] H.M. Amaro, A.C. Guedes, F.X. Malcata, Advances and perspectives in using microalgae to produce biodiesel, Appl. Energy 88 (2011) 3402–3410.
[7] S. Musharraf, M. Ahmed, N. Zehra, N. Kabir, M. Choudhary, A.-u. Rahman, Biodiesel production from microalgal isolates of southern Pakistan and quantification of FAMEs by GC – MS/MS analysis, Chem. Cent. J. 6 (2012) 149.
[8] T.M. Mata, A.A. Martins, N.S. Caetano, Microalgae for biodiesel production and other applications: a review, Renew. Sust. Energ. Rev. 14 (2010) 217–232.
[9] G. Knothe, Designer biodiesel: optimizing fatty ester composition to improve fuel properties, Energy Fuel 22 (2008) 1358–1364.
[10] G. Knothe, K.R. Steidley, Kinematic viscosity of biodiesel fuel components and related compounds. Influence of compound structure and comparison to petrodiesel fuel components, Fuel 84 (2005) 1059–1065.
[11] I.n. Barabás, I.-A. Todoru , Biodiesel Quality, Standards and Properties, Biodiesel-Quality, Emissions and By-Products, in: G. Montero, M. Stoytcheva (Eds.), InTech., 2011
[12] R. Dunn, Improving the Cold Flow Properties of Biodiesel by Fractionation, Soybean — Applications and Technology, in: T.-B. Ng (Ed.), InTech., 2011
[13] H. Wu, X. Miao, Biodiesel quality and biochemical changes of microalgae *Chlorella pyrenoidosa* and *Scenedesmus obliquus* in response to nitrate levels, Bioresour. Technol. 170 (2014) 421–427.
[14] S.K. Mandotra, P. Kumar, M.R. Suseela, P.W. Ramteke, Fresh water green microalga *Scenedesmus abundans*: a potential feedstock for high quality biodiesel production, Bioresour. Technol. 156 (2014) 42–47.
[15] M. Islam, M. Magnusson, R. Brown, G. Ayoko, M. Nabi, K. Heimann, Microalgal species selection for biodiesel production based on fuel properties derived from fatty acid profiles, Energies 6 (2013) 5676–5702.
[16] S. Vidyashankar, K. Deviprasad, V.S. Chauhan, G.A. Ravishankar, R. Sarada, Selection and evaluation of CO_2 tolerant indigenous microalga *Scenedesmus dimorphus* for unsaturated fatty acid rich lipid production under different culture conditions, Bioresour. Technol. 144 (2013) 28–37.
[17] I. Nascimento, S. Marques, I. Cabanelas, S. Pereira, J. Druzian, C. de Souza, D. Vich, G. de Carvalho, M. Nascimento, Screening microalgae strains for biodiesel production: lipid productivity and estimation of fuel quality based on fatty acids profiles as selective criteria, BioEnergy Res. 6 (2013) 1–13.
[18] J. Pratoomyot, P. Srivilas, T. Noiraksar, Fatty acids composition of 10 microalgal species, Songklanakarin J. Sci. Technol. 27 (2005) 1179–1187.
[19] S. Zhang, P.-h. Liu, X. Yang, Z.-d. Hao, L. Zhang, N. Luo, J. Shi, Isolation and identification by 18S rDNA sequence of high lipid potential microalgal species for fuel production in Hainan Dao, Biomass Bioenergy 66 (2014) 197–203.
[20] P. Prabakaran, A.D. Ravindran, Scenedesmus as a potential source of biodiesel among selected microalgae, Curr. Sci. 102 (2012) 616–620.
[21] S.-H. Ho, C.-Y. Chen, J.-S. Chang, Effect of light intensity and nitrogen starvation on CO_2 fixation and lipid/carbohydrate production of an indigenous microalga *Scenedesmus obliquus* CNW-N, Bioresour. Technol. 113 (2012) 244–252.
[22] S. Kaur, M. Sarkar, R.B. Srivastava, H.K. Gogoi, M.C. Kalita, Fatty acid profiling and molecular characterization of some freshwater microalgae from India with potential for biodiesel production, New Biotechnol. 29 (2012) 332–344.
[23] L. Xin, H. Hong-ying, G. Ke, S. Ying-xue, Effects of different nitrogen and phosphorus concentrations on the growth, nutrient uptake, and lipid accumulation of a freshwater microalga *Scenedesmus* sp. Bioresour. Technol. 101 (2010) 5494–5500.
[24] S. Mandal, N. Mallick, Microalga *Scenedesmus obliquus* as a potential source for biodiesel production, Appl. Microbiol. Biotechnol. 84 (2009) 281–291.
[25] J. Shi, B. Podola, M. Melkonia, Removal of nitrogen and phosphorus from wastewater using microalgae immobilized on twin layers: an experimental study, J. Appl. Phycol. 19 (2007) 417–423.
[26] L. Wang, Y. Li, M. Sommerfeld, Q. Hu, A flexible culture process for production of the green microalga *Scenedesmus dimorphus* rich in protein, carbohydrate or lipid, Bioresour. Technol. 129 (2013) 289–295.
[27] A. Toledo-Cervantes, M. Morales, E. Novelo, S. Revah, Carbon dioxide fixation and lipid storage by *Scenedesmus obtusiusculus*, Bioresour. Technol. 130 (2013) 652–658.
[28] S.-H. Ho, W.-M. Chen, J.-S. Chang, *Scenedesmus obliquus* CNW-N as a potential candidate for CO_2 mitigation and biodiesel production, Bioresour. Technol. 101 (2010) 8725–8730.
[29] C.A.W. Allen, K.C. Watts, R.G. Ackman, M.J. Pegg, Predicting the viscosity of biodiesel fuels from their fatty acid ester composition, Fuel 78 (11) (1999) 1319–1326.
[30] L.C. Meher, D. Vidya Sagar, S.N. Naik, Technical aspects of biodiesel production by transesterification—a review, Renewable Sustainable Energy Rev. 10 (11) (2006) 248–268.
[31] É.C. Francisco, D.B. Neves, E. Jacob-Lopes, T.T. Franco, Microalgae as feedstock for biodiesel production: carbon dioxide sequestration, lipid production and biofuel quality, J. Chem. Technol. Biotechnol. 85 (2010) 395–403.
[32] L. Grunberg, A.H. Nissan, Mixture law for viscosity, Nature 164 (1949) 799–800.
[33] L.F. Ramírez-Verduzco, J.E. Rodríguez-Rodríguez, A.d.R. Jaramillo-Jacob, Predicting cetane number, kinematic viscosity, density and higher heating value of biodiesel from its fatty acid methyl ester composition, Fuel 91 (2012) 102–111.
[34] M.J. Ramos, C.M. Fernández, A. Casas, L. Rodríguez, A. Pérez, Influence of fatty acid composition of raw materials on biodiesel properties, Bioresour. Technol. 100 (2009) 261–268.
[35] J.C. Chavarria-Hernandez, D.E. Pacheco-Catalán, Predicting the kinematic viscosity of FAMEs and biodiesel: empirical models, Fuel 124 (2014) 212–220.
[36] R.M. Carvalho Júnior, J.V.C. Vargas, L.P. Ramos, C.E.B. Marino, J.C.L. Torres, Microalgae biodiesel via in situ methanolysis, J. Chem. Technol. Biotechnol. 86 (2011) 1418–1427.
[37] E. Kessler, M. Schäfer, C. Hümmer, A. Kloboucek, V.A.R. Huss, Physiological, biochemical, and molecular characters for the taxonomy of the subgenera of *Scenedesmus* (Chlorococcales, Chlorophyta), Bot. Acta 110 (1997) 244–250.
[38] F.R. Trainor, P.F. Egan, Phenotypic plasticity in *Scenedesmus* (*Chlorophyta*) with special reference to *S. armatus* unicells, Phycologia 29 (1990) 461–469.
[39] F.R. Trainor, Biological aspects of *Scenedesmus* (Chlorophyceae) — phenotypic plasticity, in: J. Cramer (Ed.), Nova Hedwigia, 1998.
[40] S.S. An, T. Friedl, E. Hegewald, Phylogenetic relationships of *Scenedesmus* and *Scenedesmus*-like coccoid green algae as inferred from ITS-2 rDNA sequence comparisons, Plant Biol. 1 (1999) 418–428.
[41] E.J. Van Hannen, M. Lürling, E. Van Donk, Sequence analysis of the ITS-2 region: a tool to identify strains of *Scenedesmus* (Chlorophyceae), J. Phycol. 36 (2000) 605–607.
[42] D.S. Gorman, R.P. Levine, Cytochrome f and plastocyanin: their sequence in the photosynthetic electron transport chain of *Chlamydomonas reinhardi*, Proc. Natl. Acad. Sci. 54 (1965) 1665–1669.
[43] O. Perez-Garcia, F.M.E. Escalante, L.E. de-Bashan, Y. Bashan, Heterotrophic cultures of microalgae: metabolism and potential products, Water Res. 45 (2011) 11–36.
[44] S. Dellaporta, J. Wood, J. Hicks, A plant DNA minipreparation: version II, Plant Mol. Biol. Report. 1 (1983) 19–21.
[45] E. Van Hannen, P. FinkGodhe, M. Lurling, A revised secondary structure model for the internal transcribed spacer 2 of the green algae *Scenedesmus* and *Desmodesmus* and its implication for the phylogeny of these algae, Eur. J. Phycol. 37 (2002) 203–208.
[46] B. Merget, C. Koetschan, T. Hackl, F. Förster, T. Dandekar, T. Müller, J. Schultz, M. Wolf, The ITS2 Database, 612012. 3806.
[47] J. Schultz, M. Wolf, ITS2 sequence–structure analysis in phylogenetics: a how-to manual for molecular systematics, Mol. Phylogenet. Evol. 52 (2009) 520–523.
[48] P. Seibel, T. Muller, T. Dandekar, J. Schultz, M. Wolf, 4SALE — a tool for synchronous RNA sequence and secondary structure alignment and editing, BMC Bioinforma. 7 (2006) 498.
[49] M. Wolf, J. Friedrich, T. Dandekar, T. Müller, CBCAnalyzer: inferring phylogenies based on compensatory base changes in RNA secondary structures, In Silico Biol. 5 (2005) 291–294.
[50] D.H. Huson, C. Scornavacca, Dendroscope 3: an interactive tool for rooted phylogenetic trees and networks, Syst. Biol. 61 (2012) 1061–1067.
[51] A. Widjaja, C.-C. Chien, Y.-H. Ju, Study of increasing lipid production from freshwater microalgae *Chlorella vulgaris*, J. Taiwan Inst. Chem. Eng. 40 (2009) 13–20.
[52] D.Y.C. Leung, B.C.P. Koo, Y. Guo, Degradation of biodiesel under different storage conditions, Bioresour. Technol. 97 (2006) 250–256.
[53] W.E. Klopfenstein, Effect of molecular weights of fatty acid esters on cetane numbers as diesel fuels, J. Am. Oil Chem. Soc. 62 (1985) 1029–1031.
[54] R.L. McCormick, M.S. Graboski, T.L. Alleman, A.M. Herring, K.S. Tyson, Impact of biodiesel source material and chemical structure on emissions of criteria pollutants from a heavy-duty engine, Environ. Sci. Technol. 35 (2001) 1742–1747.
[55] M.J. Pratas, S. Freitas, M.B. Oliveira, S.C. Monteiro, A.S. Lima, J.A.P. Coutinho, Densities and viscosities of fatty acid methyl and ethyl esters, J. Chem. Eng. Data 55 (2010) 3983–3990.

[56] B. Freedman, M.O. Bagby, Heats of combustion of fatty esters and triglycerides, J. Am. Oil Chem. Soc. 66 (1989) 1601–1605.
[57] G. Knothe, Structure indices in FA chemistry. How relevant is the iodine value? J. Am. Oil Chem. Soc. 79 (2002) 847–854.
[58] J.-Y. Park, D.-K. Kim, J.-P. Lee, S.-C. Park, Y.-J. Kim, J.-S. Lee, Blending effects of biodiesels on oxidation stability and low temperature flow properties, Bioresour. Technol. 99 (2008) 1196–1203.
[59] E. Hegewald, Taxonomy and phylogeny of *Scenedesmus*, Algae 12 (1997) 235–246.
[60] E. Hegewald, E. Schnepf, *Scenedesmus abundans* (Kirchn.) Chod., an older name for Chlorella fuscaShih. et Krauss, Archiv für Protistenkunde 139 (1991) 133–176.
[61] L.A. Lewis, V.R. Flechtner, Cryptic species of *Scenedesmus* (*Chlorophyta*) from desert soil communities of Western North America, J. Phycol. 40 (2004) 1127–1137.
[62] E. Hegewald, K. Engelberg, R. Paschma, Beitrag zur Taxonomie der Gattung *Scenedesmus*, subgenus *Scenedesmus Chlorophyceae*, Nova Hedwigia 47 (1988) 497–533.
[63] E. Hegewald, M. Wolf, A. Keller, T. Friedl, L. Krienitz, ITS2 sequence–structure phylogeny in the Scenedesmaceae with special reference to *Coelastrum* (Chlorophyta, Chlorophyceae), including the new genera *Comasiella* and *Pectinodesmus*, Phycologia 49 (2010) 325–335.
[64] T. Müller, N. Philippi, T. Dandekar, J. Schultz, M. Wolf, Distinguishing species RNA, 132007. 1469–1472.
[65] Q. Hu, M. Sommerfeld, E. Jarvis, M. Ghirardi, M. Posewitz, M. Seibert, A. Darzins, Microalgal triacylglycerols as feedstocks for biofuel production: perspectives and advances, Plant J. 54 (2008) 621–639.
[66] Y.-Y. Pan, S.-T. Wang, L.-T. Chuang, Y.-W. Chang, C.-N.N. Chen, Isolation of thermotolerant and high lipid content green microalgae: oil accumulation is predominantly controlled by photosystem efficiency during stress treatments in *Desmodesmus*, Bioresour. Technol. 102 (2011) 10510–10517.
[67] R.A.I. Abou-Shanab, I.A. Matter, S.-N. Kim, Y.-K. Oh, J. Choi, B.-H. Jeon, Characterization and identification of lipid-producing microalgae species isolated from a freshwater lake, Biomass Bioenergy 35 (2011) 3079–3085.